Available online at www.sciencedirect.com

ScienceDirect

Physics Procedia 12 (2011) 638–645

Physics Procedia

LiM 2011

Contribution to Numerical Simulation of Laser Welding

Milan Turňa[a]*, Bohumil Taraba[b], Petr Ambrož[c], Miroslav Sahul[a]

[a]*Department of Welding, Faculty of Materials Science and Technology, Slovak University of Technology, Paulínska 16, 917 24 Trnava, Slovak Republic*

[b]*Department of Applied Mechanics, Faculty of Materials Science and Technology, Slovak University of Technology, Paulínska 16, 917 24 Trnava, Slovak Republic*

[c]*Faculty of Mechanical Engineering, Research Center of Manufacturing Technology, Czech Technical University in Prague, Horská 3, 128 00 Prague, Czech Republic*

Abstract

Contribution deals with numerical simulation of thermal and stress fields in welding tubes made of austenitic stainless CrNi steel type AISI 304 with a pulsed Nd:YAG laser. Process simulation was realised by use of ANSYS 10 software. Experiments were aimed at solution of asymptotic, standard and the so-called shell model. Thermally dependent properties of AISI 304 steel were considered. Thermal fields developed in the course of welding process and also shape of weld pool were assessed. Contribution is aimed at simulation of technological welding process with input parameters regarding the thermal and strain task and comparison of attained results with real experiment. The achieved results of numerical simulation were almost identical with a real weldment thermally affected by welding process.

Keywords: Laser Welding; Nd:YAG Laser; CrNi Stainless Steel; Finite Element Method

1. Introduction

Laser welding have become a significant technological process applicable for metallurgical joining of metallic materials [1, 2]. Besides welding also thermal cutting and heat treatment etc is concerned. In the field of industrial lasers, there are at present dominating CO_2 and solid-state systems [3]. Application of laser with a shorter wavelength is more advantageous, since it is more efficiently absorbed by the processed material [1, 4, 5]. In order to attain savings in time and costs needed for fabrication of welds, it is necessary to employ the simulation of welding process for the mentioned material.

Numerical simulation of technological processes including welding is permanently interesting subject of research and practical applications. In the National Institute of Technology Tiruchirappalli, there were compared the results of numerical simulation and real experiment in laser welding process applied on AISI 304 steel 1.6 mm in thickness. A three-dimensional, conical Gaussian heat source was used in analysis. Temperature dependent thermo-physical properties of AISI 304 steel were applied in non-linear, transient thermal analysis. Optimised welding parameters were as follows: laser power 1.25 kW and welding speed 750 $mm.min^{-1}$ at normal incidence of laser beam on the welded surface [6]. Next research deals with a numerical simulation of laser keyhole welding process with

* Corresponding author. Tel.: +421 944 373 475
E-mail address: milan.turna@stuba.sk.

1875-3892 © 2011 Published by Elsevier Ltd.
doi:10.1016/j.phpro.2011.03.080

application of control volume method [7]. Kim, K. et al. have studied the pulsed welding with Nd:YAG laser applied for joining austenitic CrNi steel type AISI 304, 1, 2 and 3 mm in thickness. Simulation was realised in a program based on the finite-element method [8]. Al-Kazzaz, H. et al. fabricated experimental welds and realised modelling of laser welding process applied on magnesium alloy type ZE41A used in aerospace industry. Welding was performed on a continuous wave Nd:YAG laser with 4 kW power. Simulation of technological welding process was realised by combination and integration of various models and concepts in order to calculate the keyhole and weld geometry profiles [9]. Rong, Y. S. et al. dealt with a numerical simulation of temperature fields in laser welding Al alloys with different thicknesses. The attained results were compared with real temperature fields that were measured by use of thermocouples [10]. Temperature fields and shape of weld pool in welding AISI 304 steel 1 mm in thickness were calculated in FLUENT program. It was concluded that the recoil pressure plays a key role in the keyhole formation, which pushes down the liquid in the weld pool and acts as the main driving force for the keyhole formation [11]. The 3-dimensional finite-element model employed in ANSYS program was created for simulating welding of AISI 304 steel by CO_2 laser with full penetration. The heat source was parameterized by the combination of a circular disk source with a Gaussian distribution of thermal flux with center on the top surface and a line source through the thickness of workpiece. The modified heat source model can predict the weld cross section in deep penetration laser welding [12]. Next research dealt with 3D finite element simulation of multi-pass welding the tube of stainless steel type AISI 316 L. The whole process included 13 weld passes and the simulation has been achieved using adaptive mesh refinements and a procedure to transport the results between the different meshes [13]. Another work dealt with laser welding of mild steel using nitrogen shielding gas. Temperature and stress fields in the weld region were computed by the finite element method. It was found out that von Mises´s stress attained high values in the cooling cycle after solidification of the molten regions. The predicted residual stress agreed well with the XRD results [14]. Finite difference method was employed to solve the governing equation and boundary conditions for obtaining fundamental information on the temperature profiles, thermal cycles, and weld pool dimensions in high-power direct diode laser welding, all which are asymmetric with respect to the weld centerline. It was caused by the fact that laser beam was tilted with an angle to the welding direction [15].

The article presents the results of numerical simulation of welding process at application of Nd:YAG laser for joining the tubes of austenitic CrNi steel type AISI 304. The attained results are compared with a real weld.

2. Experimental

Tube of austenitic CrNi steel type AISI 304 was applied as experimental material. The outer diameter of tube was Ø 52 mm and its wall thickness was 1.5 mm. From the calculated Cr and Ni equivalents and Schaeffler´s diagram [16] follows, that the structure of base metal is formed of 90 % austenite and 10 % ferrite. Chemical composition of AISI 304 steel is given in Tab. 1. The base metal was welded by a pulsed solid-state Nd:YAG laser type JK701H from Lumonics company in the „Research Center of Manufacturing Technology“ at the Czech Technical University Prague. Argon with 18 $l.min^{-1}$ flow rate was used as a shielding gas. The width of fabricated weld at its surface was 1.4 mm and at its root it was 1.15 mm.

Table 1. Chemical composition of AISI 304 steel

C [wt. %]	Mn [wt. %]	P [wt. %]	S [wt. %]	Si [wt. %]	Cr [wt. %]	Ni [wt. %]
0.08	2.0	0.05	0.03	1.0	18.0 to 20.0	8 to 10.5

The issue of laser beam welding may be defined as a dynamic, thermal and structural system, where temperature is dependent on time, while the limits are created by the initial and final state. The thermal system is designated as deterministic, continuous and non-linear. The basis of simulation model consists in knowing the welding parameters and also dimensions of welded material. At simulation of thermal tasks of laser fusion welding in ANSYS program, it is necessary to take into account that a concentrated heat source is concerned. The aim of simulation model is to verify the correctness of parameters in thermal and stress-strain task by use of ANSYS 10.0 program.

Asymptotic, standard and the so-called shell model were solved in the numerical experiment (Figure 1). Asymptotic model for thermal balance is a section of tube wall with the following dimensions: segment length: 4.74 mm, width 5.0 mm and height 1.5 mm. Owing to fact that the modelled process is symmetric from the viewpoint of

thermal loading, only half model was considered. Model volume was divided to a final number of nodal points by meshing. The selected type of element is SOLID 87, which represents a 10 point, 3D element with a quadratic basic function in ANSYS program. The generated finite-element mesh is shown in Figure 1. In the weld zone, respectively in the zone of placing thermal load, there was necessary to select a more dense mesh, owing to supposed high values of thermal gradients and thus also more dense heat flows.

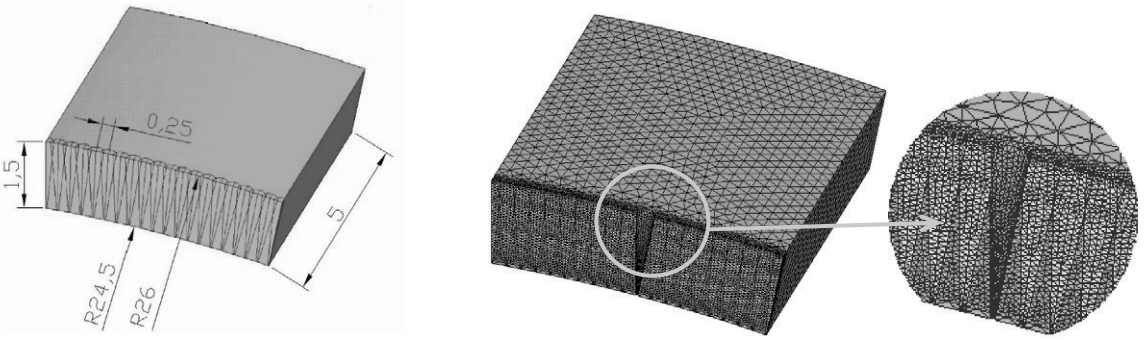

Figure 1. (a) Asymptotic model for thermal balance; (b) generated finite-element mesh

In the next stage of experimental work a circular model of tube was created in cylindrical coordinates, then meshed with application of a spatial element type brick SOLID 70. Tube volume can be divided to a mesh of elements by arbitrary angle of rotation. Rotation by 1° was selected for the solved case, what means that a mesh with 360 divisions was created.

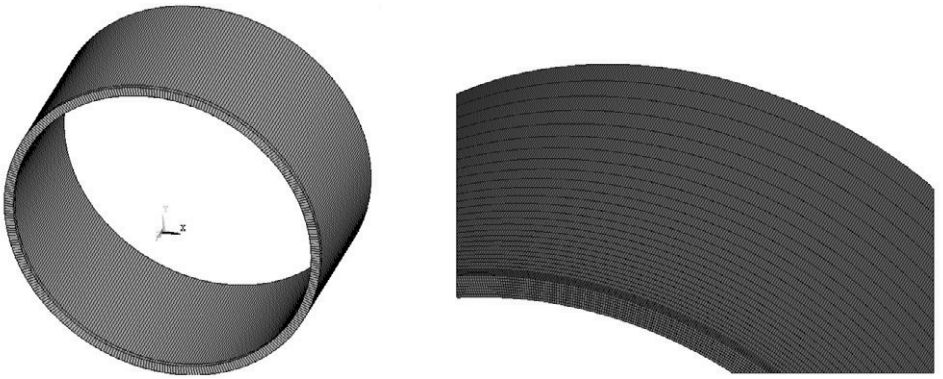

Figure 2. (a) Standard model of tube; (b) generated mesh for a standard model

Shell model (Figure 3) is characterised by a simple circumferential layer and has a defined material thickness. It is used for simulation of thin materials as replacement for the standard model.

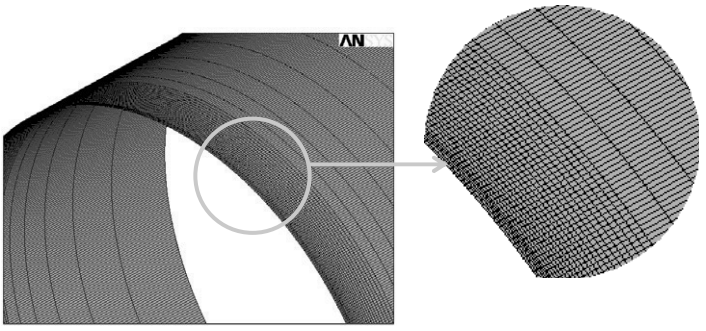

Figure 3. (a) Model of CrNi stainless tube created by the shell model method

Thermal task by the shell model method was calculated using SHELL 131 element, which is destined for solution of stationary and non- stationary thermal calculations with possibility to enter also external effects of environment on heat removal (by convection and radiation). After calculation of thermal task, for structural calculations it was then necessary to change the type of element to structural SHELL 143. Loading of the shell model was realised in the form of entering the temperature to nodal points. According to accessible literature [17] and experimental experience, the temperature in the point of beam incidence varies in interval from 2100 to 2200 °C. As a supporting program for generation of loading steps in the presented numerical experiment, Turbo Pascal software was applied.

At time 0 seconds, the initial temperature for all simulation models was entered to 20 °C. Boundary condition of 3rd type was entered for the thermal task for all surfaces that are in contact with ambient atmosphere. Rigid clamping of welded tubes is considered for the stress-strain task. All degrees of freedom are withdrawn from the nodal points located on the clamped surfaces.

Thermal loading is represented by the steps of displacing the heat source from one section to other in dependence on time. Simpler it may be said, that the thermal loading acts in defined section during the time interval Δt. Length of time section was determined from the welding speed and mesh discrediting.

Correct setting of surface loading is one of greatest problems in numerical experiment. Best proved in given case was the way of loading by entering the temperature to nodal points. Value of temperature for loading was considered from the interval of steel melting temperatures 1440 °C and sublimation temperature 2690 °C.

3. Results and Discussion

First step in numerical experiment consisted of thermal calculation, where asymptotic model was applied with entering thermal field into the keyhole surface. The keyhole shape was modelled as a rotary cone with upper diameter Ø 0.4 mm and lower diameter Ø 0.04 mm [18]. Comparison of the simulated penetration with the penetration following from macrostructure is shown in Figure 5c. Thermal field from the molten down metal is dimensionally comparable with the weld macrostructure. The mentioned comparison suggests that the calculation is correct and it corresponds to real welding conditions. At the same time it can also be stated that entering temperatures within 2100 to 2200 °C interval seems to be a correct assumption and is suitable for further applications as well.

Figure 4 shows the field of heat flow densities [$W.m^{-2}$], delivered to material by laser beam. Density of heat flow is highest on the "keyhole" wall in welding direction, namely in its tip, where it attains the value 479.10^6 $W.m^{-2}$.

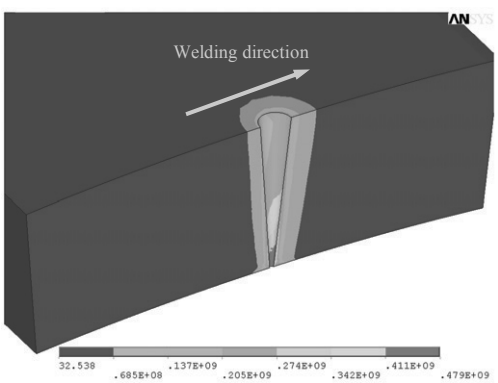

Figure 4. Field of heat flow densities on the keyhole surface

The percentage transfer of power from laser beam to weld was determined by thermal balance through a phenomenological thermodynamic analysis. During weld fabrication, 23.4 % of total laser power is necessary for molten pool formation. The balance computation serves as an informative calculation, which does not take into account the heat removal to surrounding environment and heat transfer by conduction into tube material.

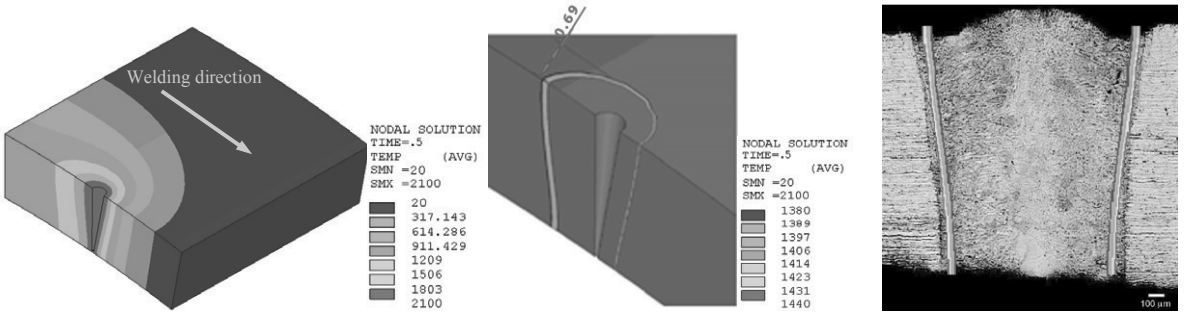

Figure 5. (a) Temperature field at time 0.5 s; (b) Welded joint zone; (c) Comparison of simulated weld with a real experiment

The shell model was selected as the most suitable and was applied for calculation of elasto-plastic tasks (structural tasks). For a simpler presentation, assessment of results is solved by use of four selected points (Figure 6) distributed over welded tube periphery (point 1 – at time t_1 = 4.9 s on weld length 26.66 mm, point 2 - at time t_2 = 12.5 s on weld length 62.54 mm, point 3 - at time t_3 = 21.1 s on weld length 105.1 mm a point 4 - at time t_4 = 27.9 s on weld length 139.6 mm). After attaining the results from thermal calculation for the shell model, these results were used as the load for the stress-strain task.

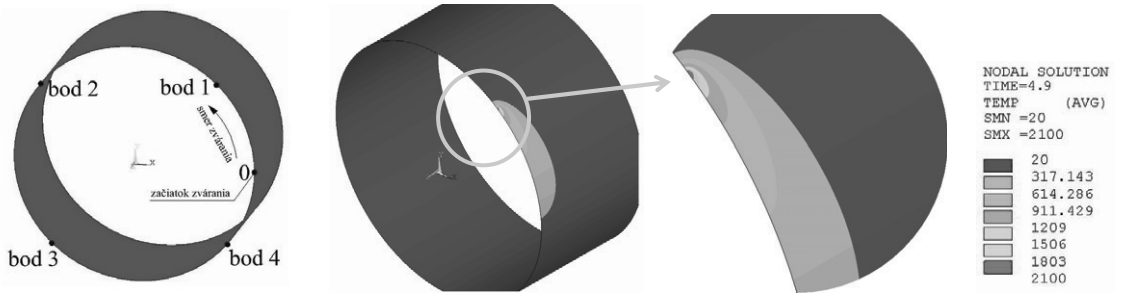

Figure 6. (a) Schematic representation of the selected points for shell model; (b) temperature field of shell model for point 1

Rigid clamping of welded parts was considered at the continuous model. Condition of symmetry was entered into weld plane.

The results of stress-strain task with an elastic material model have shown that the highest stress is formed in travel direction ahead the keyhole (Figure 7) ($\sigma_{M,max}$ = 1552 MPa). Material behaves as steady elastic and the stress ahead the keyhole and behind it attains the values above yield point (Re). This means that plastic strain will be formed in material with highest probability and also residual stresses after cooling down. At the point of laser beam acting the stress is zero, owing to presence of melt.

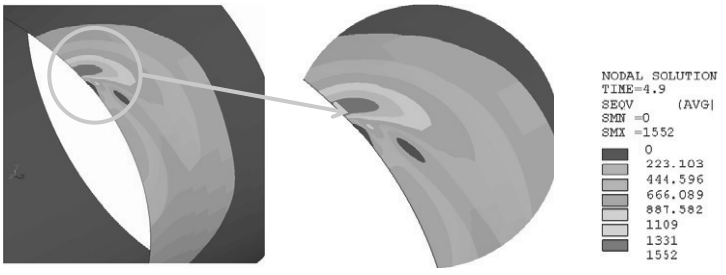

Figure 7. (a) Field of thermo-elastic equivalent Mises stresses in point 1 – continuous model with a detail of given zone

Figure 8 shows the course of Mises equivalent stresses for the selected computation points in welding direction. As concluded from graph, the stresses at selected points show very similar course and values. The highest stress is acting ahead the keyhole and shows a rapid growth.

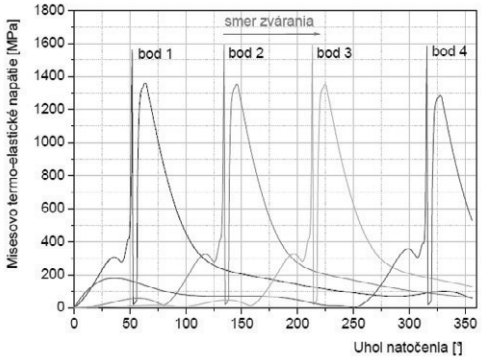

Figure 8. Dependence of Mises thermo-elastic stresses [MPa] on rotation angle [°] for the selected points 1 to 4

After fabrication of weld and solidification of weld metal the stress again rapidly increases but does not attain the value from keyhole front. With temperature drop also thermo-elastic stress decreases.

Stress-strain task for thermo-elastic discontinuous model considers real state of melt solidification in welding. It is principally aimed at preventing the expansion along the tube rotation axis in the solid phase region. Material is again clamped on both ends, what is subsequently exerted in material expansion in direction of x and y axes. In the zone of heat acting, the material is bulged. Stress field in material is distributed in different manner than at previous analysis.

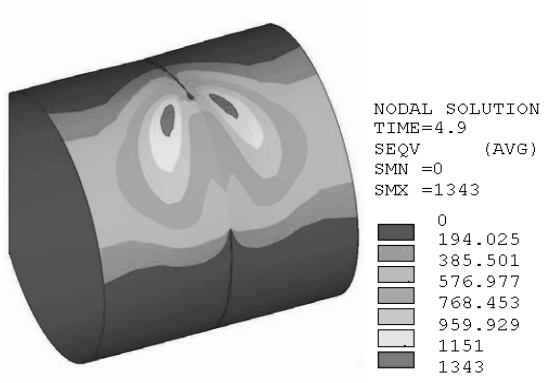

Figure 9. Field of thermo-elastic equivalent Mises stresses in point 1 for discontinuous model

At calculation of stress-strain task with application of thermo-elasto-plastic continuous model, the dependence of yield point Re [MPa] on temperature T [°C] is considered. As evident from the results attained the stresses on the level of yield point Re [MPa] occur.

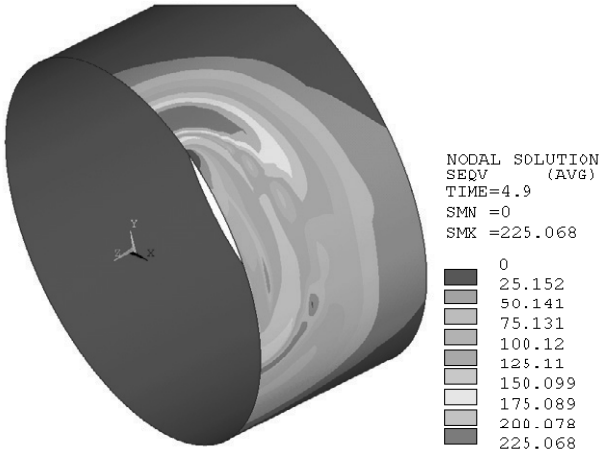

Figure 10. Field of thermo-elasto-plastic equivalent Mises stresses for point 1 – continuous model

Figure 11 shows a documented course of Mises thermo-plastic strain in welding direction and across the weld in point 1. Stress ahead the melt zone increases to 98 MPa value, it is zero in melt and after weld metal solidification it increases to 50 MPa. The course of Mises thermo-plastic strain across the weld attains maximum value 171 MPa at 4.4 mm distance from the keyhole. Steady plastic strain deformation at continuous model is formed in the weld zone and in the heat affected zone.

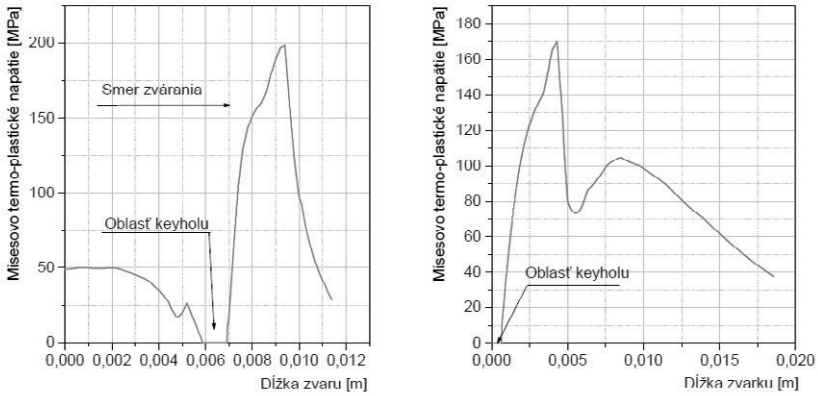

Figure 11. Mises thermo-plastic stress for a continuous model (a) in welding direction; b) across welded joint

After study of professional literature and internet resources, several possibilities of entering load were tested in this work. The method of entering heat to nodal points proved to be the most suitable. Problem occurred just at generation of load steps, since dimensions in tenths of millimetre were considered, what resulted in a great number of loading steps. This problem was solved by use of Turbo Pascal program, which cyclically generated the loading steps, subsequently imported to ANSYS program.

4. Conclusions

The aim of contribution was to develop the simulation models suitable for Nd:YAG laser welding applied for joining tubes made of CrNi austenitic stainless steel type AISI 304. The main aim of presented work was to consider the material properties of used material, determination of uniqueness conditions, selection of load, design of simulation models for the thermal and stress-strain tasks and assessment of the achieved results of welding process.

For comparison of the simulated results with results of real welding, weld macrostructure was prepared. Presented results are almost identical with a real macrostructure of weld. Informative calculation of thermal balance indicates that for weld pool formation 23.4 % power transferred from the total laser beam power is needed. Proper merit of contribution consists in defining and analysis of geometric models enabling to solve similar issues with a high probability of success also in the future.

Acknowledgements

The work was financed by aim of GA of the Slovak Republic MŠ SR and SAV (project No. 1/0842/09).

References

[1] Paschotta, R.: Encyclopedia of Laser Physics and Technology. Wiley-WCH, Weinheim, 2008.
[2] Dahotre, N. B.; Harimkar, S. P.: Laser Fabrication and Machining of Materials. Springer, New York, 2010.
[3] Trenčiansky, J.: Počítačové modelovanie tepelno-deformačného cyklu zvárania austenitických ocelí laserovým lúčom (Computer modelling of stress-strain cycle at laser welding of austenitic steels). MTF, Trnava, 2008.
[4] Ready, J. F.: LIA Handbook of Laser Materials Processing. LIA, USA, 2001.
[5] Grotte, K. H., Antonsson, E. K.: Springer Handbook of Mechanical Engineering. Springer, New York, 2009.
[6] Balasubramanian, K. R.; Siva Shanmugan, N.; Buvanashekaran, G.; Sankaranarayanasamy, K.: Numerical and Experimental Investigation of Laser Beam Welding of AISI 304 Stainless Steel Sheet. In: Advances in Production Engineering & Management 3 (2008), pp. 93-105.
[7] Wang, H.; Shi, Y.; Gong, S.: Numerical Simulation of Laser Keyhole Welding Processes Based on Control Volume Methods. In Journal of Physics D: Applied Physics 39 (2006), pp. 4722-4730.
[8] Kim, K.; Lee, J.; Cho, H.: Analysis of Pulsed Nd:YAG Laser Welding of AISI 304 Steel. In: Journal of Mechanical Science and Engineering 11 (2010), pp. 2253-2259.
[9] Al-Kazzaz, H.; Medraj, M.; Cao, X.; Jahazi, M.: Nd:YAG Laser Welding of Aerospace Grade ZE41A Magnesium Alloy: Modeling and Experimental Investigations. In: Computational Materials Science 44 (2009), pp. 858-866.
[10] Rong, Y. S.; Hui, X. J.; Ding, F.: Numerical Simulation on Temperature Field in Laser Welding for Aluminium Alloy with Different Thicknesses. In: Material Science Forum 575-578 (2008), pp. 774-779.
[11] Wang, R.; Lei, Y.; Shi, Y.: Numerical Simulation of Transient Temperature Field during Laser Keyhole Welding of 304 Stainless Steel Sheet. In: Optics & Laser Technology 43 (2011), pp. 870–873.
[12] Kazemi, K.; Goldak, J. A.: Numerical Simulation of Laser Full Penetration Welding. In: Computational Materials Science 44 (2009), pp. 841–849
[13] Duranton, P.; Devaux, J.; Robin, V.; Gilles, P.; Bergheau, J. M.: 3D Modelling of Multipass Welding of a 316L Stainless Steel Pipe. In: Journal of Materials Processing Technology 153–154 (2004), pp. 457–463.
[14] Yilbas, B. S.; Arif, A. F. M.; Abdul Aleem, B. J.: Laser Welding of Low Carbon Steel and Thermal Stress Analysis. In: Optics & Laser Technology 42 (2010), pp. 760-768.
[15] Wua, C. S.; Wanga, H. L.; Zhang, Y. M.: Numerical Analysis of the Temperature Profiles and Weld Dimension in High Power Direct-Diode Laser Welding. In: Computational Materials Science 46 (2009), pp. 49-56.
[16] Lippold, J. C.; Kotecki, D. J.: Welding Metallurgy and Weldability of Stainless Steels. John Wiley & Sons, New Jersey, 2005.
[17] Radaj, D.: Schweissprozess-simulation. Verlag für Schweissen und verwandte Verfahren DVS-Verlag GmbH, Düsseldorf, 1999.
[18] Available online: <http://info.tuwien.ac.at/iflt/theory/weldmodell/weldmodell.html>